Surface Behavior of Alumina-Supported Pt Catalysts Modified with Cerium as Revealed by X-ray Diffraction, X-ray Photoelectron Spectroscopy, and Fourier Transform Infrared Spectroscopy of CO Adsorption

Benecildo A. Riguetto,[†] Sonia Damyanova,[‡] Gias Gouliev,[‡] Clelia M. P. Marques,[†] Lachezar Petrov,[‡] and Jose Maria C. Bueno*[,§]

DQ-Universidade Federal de São Carlos and DEQ-Universidade Federal de São Carlos, Caixa Postal 676, 13565-905 São Carlos, SP, Brazil, and Institute of Catalysis, Bulgarian Academy of Sciences, 1113 Sofia, Bulgaria

Received: October 16, 2003; In Final Form: January 27, 2004

The effects of the carrier and pretreatment temperature on the oxidation state of Ce and Pt were evaluated in Pt/Al_2O_3, Pt/CeO_2, and $Pt/CeO_2-Al_2O_3$ catalyst samples with various CeO_2 loadings by applying the following spectroscopic techniques to the samples: X-ray diffraction (XRD), X-ray photoelectron spectroscopy (XPS), and Fourier transform infrared (FTIR) spectroscopy of CO adsorption. XRD showed that ceria agglomerates at high CeO_2 loadings (>3 wt %) and at a high temperature of calcination. XPS spectra showed that Ce(III) is formed more easily in the presence of Pt caused by the electron transfer between Pt and CeO_2. A variation in the intensity and a shift in the IR bands from CO adsorbed on reduced Pt were observed, as a function of the temperature of reduction and type of the support. A heterogeneous distribution of linearly adsorbed CO on Pt at terraces and defect sites was proposed for Pt/Al_2O_3 reduced at the lower temperature (623 K), while at the higher temperature of reduction (773 K) a complete reduction of the Pt was observed. The higher reduction temperature and increasing the CeO_2 loading led to a more uniform distribution of Pt on $Pt/CeO_2-Al_2O_3$, related to the presence of highly unsaturated Pt caused by the strong interaction between Pt and Ce-modified alumina. The electronic effect dominates in Pt/CeO_2 samples reduced at very high temperature (973 K).

1. Introduction

Transition metals supported on cerium-based supports have revealed interesting properties in numerous catalytic reactions, most of them related to the catalytic cleaning of exhaust gases from internal combustion engines,[1−3] removal of SO_x from fluid catalytic cracking (FCC) fuel gases,[4,5] and reforming of natural gas.[6−10] The wide application of ceria as a catalyst or as an additive to different catalysts is mainly due to both (i) its unique acid−base and redox properties[3] and (ii) its low cost. Although a large number of papers have been dedicated to the study of the surface properties of compounds of rare-earth elements with fluorite structure, as reference compounds or as additives to supported noble metal (Pt, Rh, Pd) catalysts, the major questions concerning their influence on the electronic state of the active metal are still a subject of discussion in the literature.

Different techniques have been used to characterize noble metals supported on cerium oxide: transmission electron microscopy (TEM),[10−12] Fourier transform infrared (FTIR) spectroscopy,[13−16] H_2 chemisorption,[10,11] X-ray photoelectron spectroscopy (XPS),[17,18] temperature-programmed reduction (TPR),[19,20] etc.

It is well-known that carbon monoxide is a useful probe molecule for characterization of the surface properties of metals and metal oxides via adsorption. On the other hand, CO adsorption is especially related to the study of reactions involving CO itself, such as CO hydrogenation, CO oxidation, and reforming of methane reactions. During catalytic reaction a mixture of different species covers the surface of the working catalyst: initial reactants, reaction products, and various intermediate surface compounds. Therefore, it is very important to study the adsorption processes of these chemical compounds and the properties and behavior of the adsorbed species. However, it is well-known that the dissociative adsorption of CO on the catalyst surface leads to formation of the coke precursors. To obtain information on the nature of the surface species on various catalysts, much work[21−24] has been dedicated to the study of CO adsorption on different metal oxides by IR spectroscopy.

The present work is a continuation of the study of supported noble metal catalysts for use in the reforming of natural gas in our laboratories.[25−27] Adsorbed CO probe molecules were used to characterize the electronic state and the surface Pt sites present on catalysts supported on $CeO_2-Al_2O_3$. To our knowledge this work is the first attempt to characterize Pt supported on mixed $CeO_2-Al_2O_3$ oxides by infrared spectroscopy of CO adsorption, since most other studies have concentrated on the study of Pt supported on single oxides such as Al_2O_3, TiO_2, and SiO_2. An attempt has been made to discuss to what extent the spectroscopic methods used can give a description of the oxidation state of Ce and Pt in such complex materials as $Pt/CeO_3-Al_2O_3$ catalysts, and to correlate the IR results obtained during CO adsorption with XPS studies, to distinguish between electronic effects and the effects of particle morphology. To characterize the supported Pt catalysts, the following techniques were used: FTIR of CO adsorption, XPS and X-ray diffraction (XRD).

[†] DQ-Universidade Federal de São Carlos.
[‡] Bulgarian Academy of Sciences.
[§] DEQ-Universidade Federal de São Carlos.

10.1021/jp031167s CCC: $27.50
Published on Web 04/06/2004

TABLE 1: Chemical Analysis and XPS Parameters for Calcined and Reduced Supported Pt Samples

sample	$[CeO_2]$ (wt %)	S_{BET} (m^2/g)	BE (eV) Ce $3d_{5/2}$	BE (eV) Pt $4d_{5/2}$	Pt/Ce	Pt/Al
$Pt/0.5CeO_2-Al_2O_3$	0.49	199	881.9 (882.0)[a]	315.2 (314.5)	0.864 (0.789)	0.025 (0.032)
$Pt/1CeO_2-Al_2O_3$	0.95	205	881.9 (882.0)	315.2 (314.3)	0.823 (0.646)	0.024 (0.019)
$Pt/3CeO_2-Al_2O_3$	2.92	196	881.9 (882.0)	315.0 (314.3)	0.765 (0.401)	0.016 (0.009)
$Pt/6CeO_2-Al_2O_3$	5.62	180	882.5 (882.0)	315.4 (314.6)	0.619 (0.350)	0.011 (0.005)
$Pt/12CeO_2-Al_2O_3$	10.34	162	881.9 (882.0)	315.7 (314.40)	0.513 (0.315)	0.036 (0.022)
Pt/Al_2O_3				315.2 (314.1)		
Pt/CeO_2			882.2 (882.0)	315.7 (314.6)	0.409 (0.222)	
$12CeO_2-Al_2O_3$ carrier	10.34		881.9 (881.8)			

[a] Data for reduced samples are in parentheses.

2. Experimental Section

2.1. Sample Preparation. The $CeO_2-Al_2O_3$ carriers with various CeO_2 loadings were prepared by impregnation of γ-alumina (Engelhard, $S_{BET} = 205$ m^2/g) with an aqueous solution of diammonium hexanitrate cerate, $(NH_4)_2[Ce(NO_3)_6]$ (99.99% pure product from Aldrich), as described previously in ref 28. CeO_2 carrier was obtained by calcination of $(NH_4)_2[Ce(NO_3)_6]$ at 923 K in a flow of synthetic air for 2 h. Pt/Al_2O_3, Pt/CeO_2, and $Pt/CeO_2-Al_2O_3$ samples were prepared by impregnation of the corresponding carriers with a solution of $H_2PtCl_6 \cdot 6H_2O$ (Degussa) in ethanol. The appropriate amount of chloroplatinic acid was dissolved in ethanol, and the support material was then added. After the mixture was stirred for 1 h at room temperature, ethanol was removed by a Rotavapor at 343 K. The samples were dried at 333 K overnight and calcined at 773 and 1073 K for 2 h in air. For all samples, the amount of Pt was about 1 wt %. The prepared samples were referred to as Pt/Al_2O_3, Pt/CeO_2, $Pt/xCeO_2-Al_2O_3$, where x is the theoretical CeO_2 content (0.5, 1, 3, 6, and 12 wt %).

2.2. Characterization. Chemical analysis was obtained by inductively coupled plasma atomic emission spectroscopy (ICP-AES). The sample compositions are summarized in Table 1.

X-ray diffraction spectra of the samples were collected with a Rigaku DMAX 2500 PC diffractometer, using Cu Kα radiation. The step scans were taken over a range of 2θ from 10° to 75° in steps of 0.020°, and the intensity data for each one were collected for 10 s.

X-ray photoelectron spectra were obtained with an ESCALAB II, VG Scientific, spectrometer with a monochromatic Al Kα source ($E = 1487$ eV). The samples were pressed into pellets and reduced in situ with H_2 in the pretreatment XPS chamber. The residual pressure inside the analysis chamber was below 1×10^{-9} Torr. The binding energies (BEs) of O 1s, Ce 3d, Pt 4d, and Al 2p were determined by a computer fitting of the measured spectra and were referenced to the C 1s band at 284.6 eV. The binding energies were estimated with accuracy within ± 0.2 eV. The surface atomic ratios were calculated as ratios of the corresponding peak intensities, corrected with theoretical sensitivity factors based on Scofield's photoionization cross sections.[29]

Infrared spectra of 4 cm^{-1} resolution were recorded by a Nicolet Magna 750 FTIR spectrometer with a diffuse reflectance cell and a DRIFT reactor cell with ZnSe windows (Spectra Tech), using 128 scans for each spectrum. The adsorption by the windows and by the blank powdered sample was subtracted from all the spectra. Prior to CO adsorption, the samples were reduced under a flow of H_2 for 20 min at 623 or 773 K in a fixed-bed reactor. After that the reactor was cooled to room temperature. The undiluted sample was placed in a DRIFT cell and purged in a flow of nitrogen overnight. The samples were reduced at 623, 773, or 973 K in a mixture of H_2:N_2 = 1:3 flowing at 50 mL/min for 2 h, heating to 623 or 773 K at 10 K/min. The samples were cooled to room temperature in a N_2 flow, followed by CO being introduced into the DRIFT cell by pulses at various CO pressures and 300 K, and the first spectrum was then recorded for each sample. CO desorption measurements were performed by heating of the samples at different temperatures in a N_2 flow.

3. Results

3.1. XRD Data. XRD patterns of reduced Pt/Al_2O_3, Pt/CeO_2, and $Pt/CeO_2-Al_2O_3$ samples with different CeO_2 loadings, previously calcined at 773 or 1073 K, are shown in parts A and B, respectively, of Figure 1. The XRD patterns of the same samples reduced at 773 K are also shown in Figure 1C. As is seen from Figure 1A any diffraction peaks of crystalline CeO_2 are not observed for samples with $[CeO_2] \leq 3$ wt % calcined at lower temperature (773 K). The CeO_2 fluorite structure,[30] with diffraction lines at $2\theta = 28.5°$, 33.3°, 47.5 °, and 56.4°, is observed in samples with $[CeO_2] \geq 6$ wt %. Calcination of the samples at 1073 K leads to a progressive crystallization of CeO_2 (Figure 1B), as well as to agglomeration of Pt particles, evident in line at $2\theta = 39.9°$, especially in the samples with lower CeO_2 loading (≤ 3 wt %) and in Pt/Al_2O_3. The agglomeration of Pt is, most probably, due to the decomposition of surface $[Pt^{IV}(O-H)_xCl_y]_s$ or $[PtO_xCl_y]_s$ species formed during calcination of the sample impregnated with the chlorine-containing precursor salt according to Lietz et al.[31] It should be noted that Pt/CeO_2 did not show any peak assigned to agglomerated Pt, while $Pt/CeO_2-Al_2O_3$ with the highest CeO_2 loading (12 wt %) showed a very small peak (Figure 1B). All reduced samples previously calcined at 773 K did not show peaks of crystallized Pt (Figure 1C), meaning that Pt is well dispersed on the surface of reduced samples.

3.2. XPS Analysis. XPS spectra of Ce 3d core electron levels for $12CeO_2-Al_2O_3$ carrier, Pt/CeO_2, and $Pt/CeO_2-Al_2O_3$ samples with varying CeO_2 loadings after calcination and reduction at 773 K are shown in parts A and B, respectively, of Figure 2. The BE values of Ce $3d_{5/2}$ and Pt $4d_{5/2}$ core electrons are summarized in Table 1. The XPS spectrum of bulk CeO_2 is complex, consisting of six components, corresponding to three pairs of spin−orbit doublets: v represents the Ce $3d_{5/2}$ contribution, and u represents the Ce $3d_{3/2}$ contribution. Binding energies at 881.5, 887.5, and 897.5 eV correspond to v, v^{II}, and v^{III} components, respectively, which are in good agreement with reported literature spectra.[32−33] Binding energies at 899.7, 906.2, and 915.6 eV correspond to u, u^{II}, and u^{III}, respectively. According to Fujimori[34] the peaks v^{III} and u^{III} have been attributed to the final state $3d^94f^0$. It is important to note that these lines are not observed with pure trivalent ionic or metallic cerium compounds.[35,36] The broader v^{II} feature is characteristic of cerium in the oxidation state of IV (Figure 2).

It is seen that XPS spectra of samples of Pt supported on $CeO_2-Al_2O_3$ oxides are different from that of pure CeO_2, and depend on the CeO_2 loading as well as on the presence of Pt. The broadening of the XPS lines for oxide samples with lower CeO_2 loading (0.5−1 wt %) suggests the presence of several surface cerium oxide species; a new weak band (v^I) at about

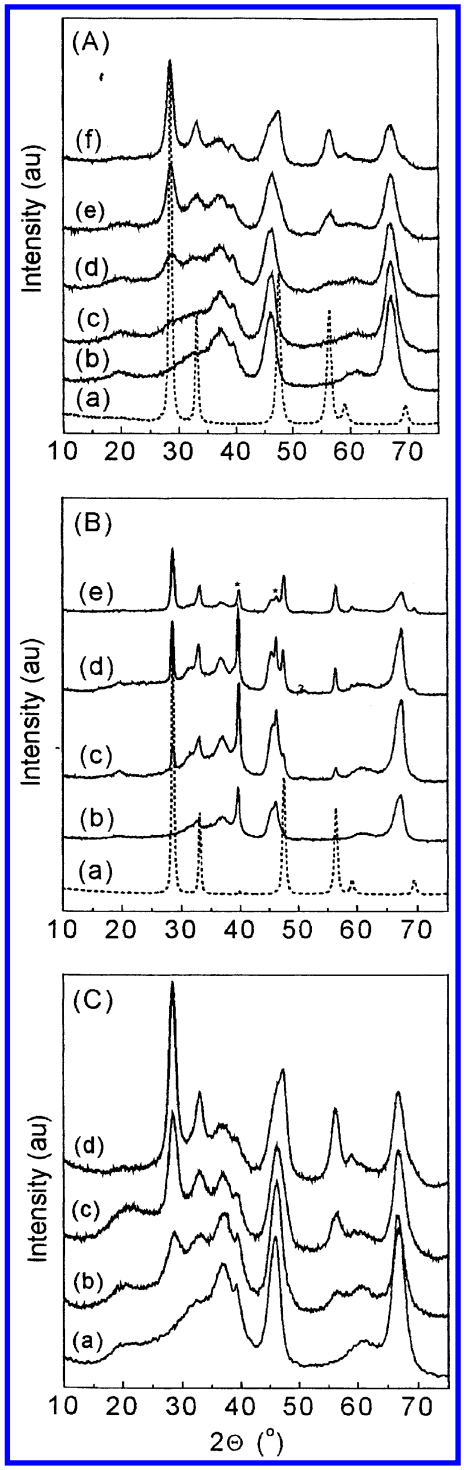

Figure 1. XRD spectra of Pt/CeO_2 and $Pt/CeO_2-Al_2O_3$ samples with different CeO_2 loadings calcined at 773 K (A) and 1073 K (B) and reduced at 773 K (C). (A) Pt/CeO_2 (a); Pt/Al_2O_3 (b); $Pt/CeO_2-Al_2O_3$: 1 (c), 3 (d), 6 (e), and 12 (f) wt % CeO_2. (B) Pt/CeO_2 (a); Pt/Al_2O_3 (b); $Pt/CeO_2-Al_2O_3$: 3 (c), 6 (d), and 12 (e) wt % CeO_2. (C) Pt/Al_2O_3 (a); $Pt/CeO_2-Al_2O_3$: 3 (b), 6 (c), and 12 (d) wt % CeO_2.

885.1 eV appears in these samples (Figure 2A). The increasing intensity of the v^I band and disappearance of v^{II} with increasing CeO_2 loading (up to 3 wt %) suggests that the oxidation state of cerium is different from IV. The energy separation between the v and v^I peaks is about 3.0 eV, close to the values observed for Ce(III) compounds.[37] For all CeO_2-containing samples a positive shift in the BE of Ce $3d_{5/2}$ (v) and Ce $3d_{3/2}$ (u^{III}), compared to those for bulk CeO_2, is observed (from 881.5 to 882.1 eV and from 915.6 to 916.1 eV for v and u^{III} peaks,

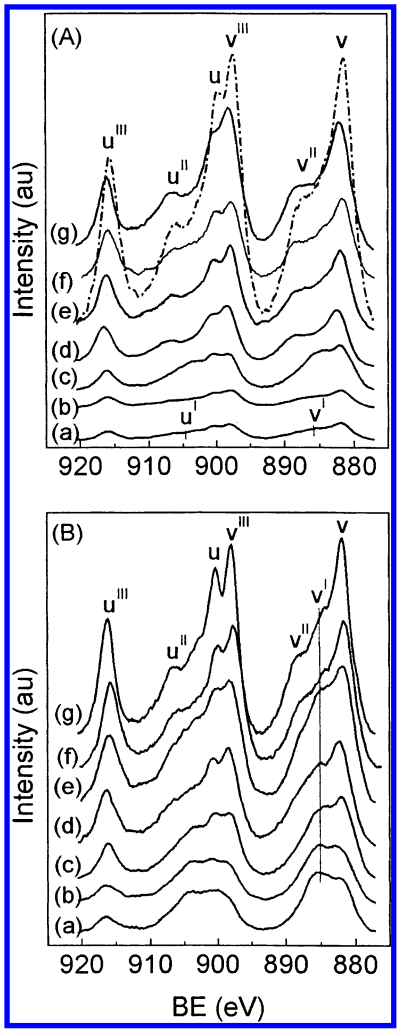

Figure 2. XPS spectra of Ce 3d core electron levels for Pt/CeO_2 and $Pt/CeO_2-Al_2O_3$ samples with different CeO_2 loadings (wt %) after calcination (A) and reduction (B) at 773 K: 0.5 (a); 1 (b); 3 (c); 6 (d); 12 (e); $CeO_2-Al_2O_3$ carrier with 12 wt % CeO_2 (f) and Pt/CeO_2 (g). Dashed lines correspond to bulk CeO_2.

respectively), which would be related to an electron transfer between CeO_2 and alumina support, as well as between CeO_2 and Pt. It should be noted that cerium on the surface of Pt-containing $CeO_2-Al_2O_3$ oxide samples is in a more reduced state than the cerium in the samples without Pt.[28] Since traces of Cl^- ions were detected by XPS in the samples calcined at 773 K, it can be concluded that cerium reacts on the surface with chlorine coming from the precursor of the transition metal and form oxychloride ($Ce^{III}OCl$) or hydroxychloride (Ce(III)-$(OH)_2Cl$) according to ref 38, which are stable up to a high temperature of calcination. On the other hand, as we discussed in our previous work[28] cerium is atomically dispersed on the surface of alumina at $[CeO_2] \leq 3$ wt %, due to the strong Ce−O−Al bond, which stabilizes cerium in the lower oxidation state. The strong interaction between cerium and alumina results in the formation of $CeAlO_3$.[39] Another type of species detected in low-CeO_2-loaded samples is well-dispersed nano-CeO_2 crystallites, this being supported by the absence of XRD lines (Figure 1A). These CeO_2 crystallites begin to grow with increasing CeO_2 loading (>3 wt % CeO_2, Figure 1A); at a higher temperature of calcination (1073 K) the particle size increases (Figure 1B).

The XPS spectra of Ce 3d core electrons in reduced $Pt/CeO_2-Al_2O_3$ samples are different from those of bulk CeO_2 and their oxide partners (Figure 2B). With higher-CeO_2-loaded samples ($[CeO_2] \geq 6$ wt %), the v^{II} peak practically disappears after

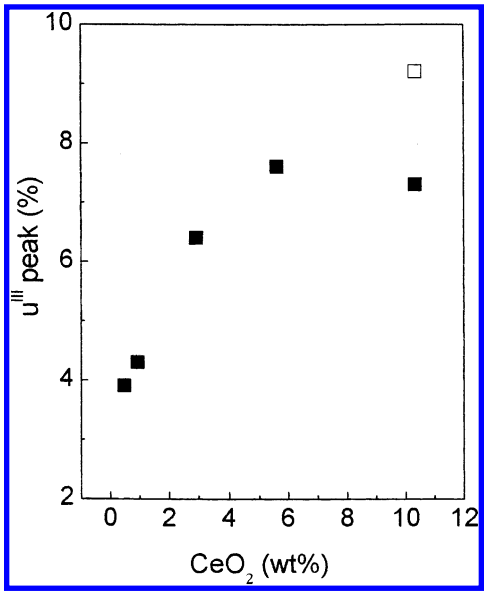

Figure 3. Percent area under the u^{III} peak as a function of CeO_2 loading in $Pt/CeO_2-Al_2O_3$ samples. The open square corresponds to $CeO_2-Al_2O_3$ carrier with 12 wt % CeO_2.

reduction and a weak peak at 884.5 eV appears, which should be assigned to metallic cerium according to Normand et al.[40] However, it is difficult to separate the poorly screened line of metallic cerium from ionic Ce(III) compounds, for samples with higher CeO_2 loading. Traces of the v^{II} peak are observed with the reduced Pt/CeO_2 sample, meaning that not all Ce(IV) is reduced. For the samples with lower CeO_2 loading (0.5−3 wt %), where cerium is already in a partially reduced calcined form, the reduction leads to an increase in the intensity of the v^{I} line. The relative intensity of the v^{I} peak is higher than of the v peak, indicating a higher contribution of Ce(III) compounds in low-CeO_2-loaded samples.

The difference between the chemical states of Ce in calcined and reduced samples is mainly due to the chemical transformation of the CeO_2/Al_2O_3 system into $CeAlO_3/Al_2O_3$. The percent area of the u^{III} peak in the total Ce 3d region (Ce $3d_{5/2}$ and Ce $3d_{3/2}$) is taken as the relative amount of Ce(IV) in each sample. A plot of this area in the Ce 3d region as a function of CeO_2 loading in the samples is shown in Figure 3. In comparison to calcined samples a significant reduction of the percentage of u^{III} occurred after reduction of the samples at 773 K in a flow of H_2 (10%)/N_2. In Figure 3 it is seen that the percentage of u^{III} increases with increasing CeO_2 loading, which means an increase in the relative amount of Ce(IV). It is interesting to note that the percentage of u^{III} for $CeO_2-Al_2O_3$ carrier is higher than in the Pt-containing sample with the same CeO_2 loading, supporting the idea that the presence of Pt leads to a lighter reduction of cerium.

It should be mentioned that it was difficult to analyze the Pt 4f lines, because of the overlap with Al 2p lines in the region around 70−80 eV and the low Pt concentration, except for the Pt/CeO_2 sample. Therefore, it was necessary to perform a very accurate determination of the binding energy values from the broad Pt 4d line. The data in the literature concerning the oxidation of Pt are contradictory,[41−43] which can be related to the different methods of preparation of supported Pt samples, i.e., the salt of the metal precursor, its metal loading, and the type of XPS equipment. An oxidation state of IV was found by Shyu and Otto[41] in PtO_2 (BE = 317.0 eV) after calcination of Pt/Al_2O_3 at 1073 K, while for Pt/CeO_2, calcined at the same temperature, the authors observed Pt in a lower oxidation state: Pt(II) in PtO (BE = 315.3 eV). In zeolite-supported Pt catalyst[42] Pt(II) ions at cationic sites with BE = 316.8 eV have been found. Jackson et al.[43] have found BEs of 317.7 eV for $PtCl_4$ and 316.2 eV for $PtCl_2$ in fresh Pt/Al_2O_3 catalyst. The BE of Pt $4d_{5/2}$ for the oxide samples is in the range of 315.0−315.7 eV (Table 1) characteristic for oxidized Pt species. It is seen that the BE values in the literature for nondispersed $PtCl_2$ or $PtCl_4$ are higher than those observed for the fresh samples calcined at 773 K. This is, possibly, due to the small Pt−Cl clusters dispersed on the supports, where chlorine is bound to the support. We can suppose that on the surface of the samples calcined at 773 K there is Pt in both oxidation states, caused by (i) the strength of the interaction with chlorine ions, which are still present at 773 K, and (ii) the electron transfer between Pt and CeO_2. The highest BE value is obtained for Pt in the Pt/CeO_2 sample, showing that Pt is in a higher oxidation state.

For all reduced samples the BE values of Pt $4d_{5/2}$ are in the range of 314.1−314.6 eV. The values are slightly higher compared to that for the completely reduced state,[41] Pt^0 (313.5 eV), on the surface of the sample, which means that Pt maintains some $\delta+$ character. The difference of 0.5 eV in the BE of Pt $4d_{5/2}$ between Pt/CeO_2 and Pt/Al_2O_3 samples suggests that Pt on alumina is more easily reduced. The fact that no Pt phase was detected by XRD in the samples reduced at 773 K suggests that all of the platinum is well dispersed on the surface of the reduced samples. According to ref 41 in reduced samples, the particulate phase, where Pt particles are bigger, exhibits a BE corresponding to Pt metal, while the dispersed phase can be recognized from the 1.0 eV higher BE. The platinum clusters probably gradually become metallic in character when the particulate phase is formed. In addition, XPS data showed that, after reduction at 773 K, traces of Cl^- ions remain on the samples, probably due to the stable Al−Cl and Ce−Cl complexes.[44]

The XPS atomic ratios of Pt/Ce and Pt/Al for calcined and reduced supported Pt samples are listed in Table 1. It can be seen that the values for Pt/Ce ratios are significantly higher than those of Pt/Al, suggesting a more intimate contact between Pt and Ce. The values of both ratios decrease after reduction. The decrease in the XPS metal/support ratio after reduction has been related to the change in the shape of the particle according to ref 43. The Pt/Ce ratios decrease with increasing CeO_2 loading. The lowest Pt dispersion is observed for the Pt/CeO_2 sample, most probably caused by the very low surface area of the CeO_2 support.[28] Pt/Al ratios decrease with increasing CeO_2 loading up to 6 wt %; after that, the Pt/Al increases significantly at 12 wt % CeO_2 due to the agglomeration of CeO_2 crystallites (Figure 1) and the surface of alumina becomes freer. It has been shown[39] that Pt interacts preferentially with Ce even in the presence of a much larger Al_2O_3 surface.

3.3. IR Results. *3.3.1. IR Spectra of CO Adsorption in the Region 1800−1000 cm^{-1}.* The IR spectra of CO adsorbed on pure CeO_2 in the region 1800−1000 cm^{-1}, which was reduced at 623 and 773 K at different pressures, are shown in parts A and B, respectively, of Figure 4. Exposure to 0.665 kPa of CO on the sample reduced at 623 K (Figure 4A) gave two rather wide bands at 1611 and 1296 cm^{-1}; each band has unresolved components, at 1587 and about 1235 cm^{-1}. The intensity of all these bands increases with increasing CO pressure, up to 5.32 kPa. Exposure to 0.665 kPa of CO on CeO_2 reduced at 773 K gave main bands at 1576 cm^{-1} with a component at about 1560 cm^{-1} and at 1295 cm^{-1} with a shoulder at about 1270 cm^{-1} (Figure 4B). Subsequent exposure to 1.33 kPa of CO yields bands at 1606 (shoulder), 1582, 1507, 1295, and 1216 cm^{-1}

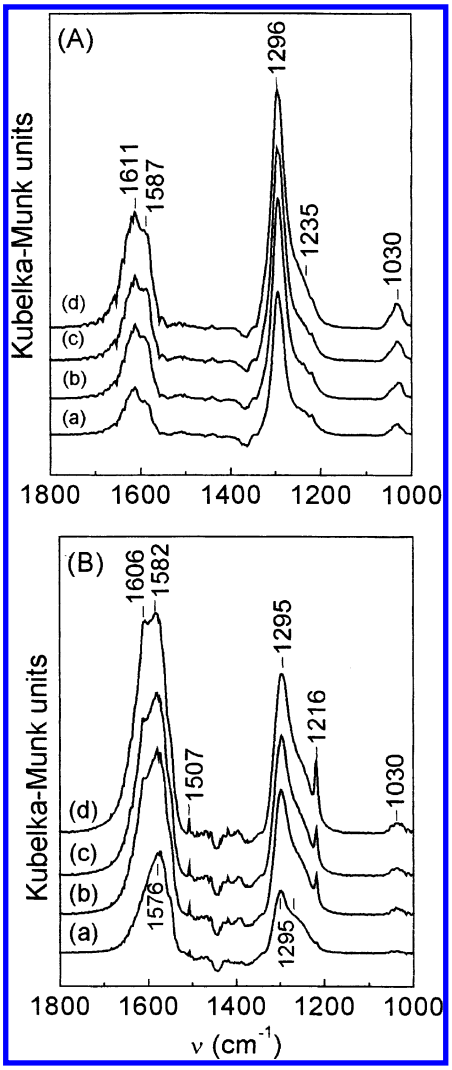

Figure 4. IR spectra of CO adsorption on CeO_2 reduced at 623 K (A) and 773 K (B) in the region of 1800−1000 cm^{-1} under different CO pressures: 0.665 (a), 1.33 (b), 2.00 (c), and 2.66 (d) kPa.

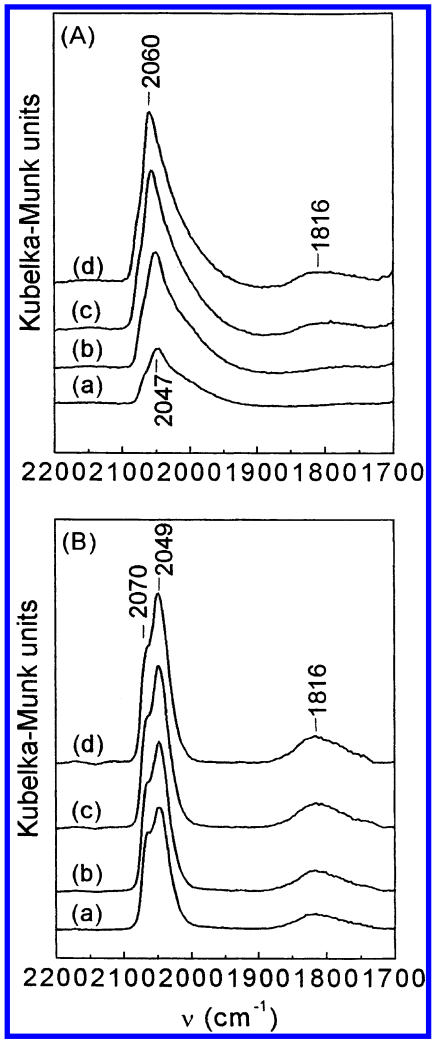

Figure 5. IR spectra of CO adsorption on Pt/Al_2O_3 reduced at 623 K (A) and 773 K (B) under different CO pressures: 0.665 (a), 1.33 (b), 2.00 (c), and 2.66 (d) kPa.

and a small one at about 1030 cm^{-1}. The relative intensity of the shoulder at about 1606 cm^{-1} increases relative to that of the 1580 cm^{-1} band, as pressure increases, and there is also a general rise in the intensities of all bands. It should be noted that the bands at 1582 and 1295 cm^{-1}, which dominate the spectra, grow at the same rate with increasing CO pressure. The change in the intensity of the bands at 1507 and 1216 cm^{-1} is different from that of the other bands; there is a very small increase in the intensity as a function of CO pressure. The bands in the region 1800−1000 cm^{-1} have been attributed to the formation of a large number of different carbonate species on the ceria surface.[45,46] The wavenumbers of the observed bands are approximately similar to those reported by other authors,[46] which have been assigned to the following adsorbed species: hydrogen carbonate (1612−1606 and 1216 cm^{-1}), bidentate carbonate (1590−1583 and 1295 cm^{-1}), polydentate carbonate (1030 cm^{-1}).

3.3.2. IR Spectra in the Region 2200−1700 cm^{-1}. The IR spectra of CO adsorbed on the Pt/Al_2O_3 sample in the region 2200−1700 cm^{-1}, which was reduced at 623 and 773 K at different pressures, are shown in parts A and B, respectively, of Figure 5. Adsorption of CO on Pt/Al_2O_3 reduced at 623 K under 0.665 kPa of pressure produces one main band at 2047 cm^{-1}, with significant broadening on the low-frequency side, and a shoulder at about 2070 cm^{-1}. Increasing CO pressure leads to (i) an increase in the intensity of the main band and of the shoulder at 2070 cm^{-1}, (ii) a shift of the main band to higher wavenumbers at ≥2.0 kPa (from 2047 to 2060 cm^{-1}), and (iii) the appearance of a small band at about 1816 cm^{-1}. After reduction of Pt/Al_2O_3 at 773 K, all spectra show a main band at 2049 cm^{-1} with a clearly-resolved shoulder at 2070 cm^{-1} and a broad band at 1816 cm^{-1}. The intensities of the bands at 2049 and 2070 cm^{-1} simultaneously increase with increasing CO pressure.

From Figure 5, it is clear that the effects of increasing the reduction temperature up to 773 K and/or raising the CO pressures on the position and intensity of CO bands for the Al_2O_3-supported Pt sample are (i) the main band shifts to a lower frequency of 2049 cm^{-1}, (ii) the shoulder on the low-frequency side of the main band is not detected, (iii) a small and broad band at about 1816 cm^{-1} is present at all CO pressures, and (iv) the intensity of all bands rises; i.e., the coverage of Pt sites by adsorbed CO increases with CO pressure. According to the observations in the literature,[21,47,48] the bands in the higher-frequency region 2100−1950 cm^{-1} and in the lower-frequency region 1900−1700 cm^{-1} (Figure 2) can be related to CO linearly bonded to one Pt and CO bonded on two surface Pt atoms (bridged species), respectively. The latter vibration contributes less than 5% to the overall absorption: as a consequence, this band is hardly detected in the case of poorly dispersed Pt. The origin of the modification of the main band could be caused by

reconstruction of the surface of the platinum particles in the presence of CO, as has been proposed by Dulaurent et al.[49] Xu and Yates[50] have shown that similar quantities of linear and bridged CO species (by TPD analysis) lead to an IR spectrum with a strong band for the linear species and a weak band for the bridged species, owing to a dipole-coupling effect. The shoulder at about 2080 cm^{-1}, for the sample reduced at low temperature, would be attributed to linear CO species adsorbed on platinum atoms existing in arrays, possibly strongly interacting with the surface of alumina.

The spectra of CO, adsorbed on Pt/CeO_2 reduced at 623, 773, and 973 K under various CO pressures, are shown in parts A−C, respectively, of Figure 6. The spectra at 623 and 773 K show two not well-resolved bands at 2087 and 2070 cm^{-1}, related to CO linearly bonded to surface-exposed metal Pt atoms. A band at 1840 cm^{-1}, associated with bridge-bonded CO species, appeared in all spectra for the sample reduced at 623 K, but practically disappeared at a higher temperature of reduction. The intensities of the strong bands varied with a change of both the temperature of reduction and the CO pressure. A shift of the low-frequency band to higher wavenumbers (to 2076 cm^{-1}) as well as a new very small band at 2119 cm^{-1} appeared in the spectra after reduction of the samples at 973 K. Since the vibrational frequency of adsorbed CO is higher when the state of metal is more positive, the band at 2119 cm^{-1} would be due to CO linearly adsorbed on Pt atoms interacting with oxygen; i.e., Pt atoms are in a more unsaturated coordination state ($Pt^{\delta+}$), probably created by a strong metal−support interaction (SMSI) at the very high temperature of reduction.[51]

The IR spectra of CO adsorbed on Pt supported on mixed $CeO_2-Al_2O_3$ carriers, with different CeO_2 loadings, reduced at 623 and 773 K, are shown in parts A and B, respectively, of Figure 7. For comparison, the spectra of Pt/Al_2O_3 samples are included. The spectra of Pt/Al_2O_3, $Pt/3CeO_2-Al_2O_3$, and $Pt/12CeO_2-Al_2O_3$ samples previously calcined at 1073 K, and after that reduced at 773 K, shown in Figure 7C; the pressure of CO adsorption is the same for all samples (2.66 kPa). In the spectrum of the sample with the lowest CeO_2 loading (0.5 wt %) and reduced at 623 K, a main band is seen at 2065 cm^{-1} (Figure 7A). The main IR band is shifted to lower wavenumbers (to 2056 cm^{-1}) with increasing CeO_2 loading (from 1 to 6 wt %) in the samples. No shift is observed for the sample with the highest CeO_2 loading (2065 cm^{-1}). All bands show broadening on the low-frequency side as well as a poorly resolved shoulder on the high-frequency side; the full width at half-maximum (fwhm) of the bands increases with increasing CeO_2 loading (Figure 7A).

Similar bands are observed in all IR spectra of CeO_2-containing Pt/Al_2O_3 samples reduced at 773 K (Figure 7B): (i) a main band is present at 2063−2065 cm^{-1}, with higher intensity and more symmetric than the bands for samples reduced at 623 K; (ii) no well-resolved high-frequency shoulder at about 2077 cm^{-1} is revealed, whose intensity compared to that of the main band increases with increasing CeO_2 loading; (iii) a band at about 1835 cm^{-1} is present at the highest CeO_2 loading (12 wt %); (iv) at CeO_2 loadings between 3 and 6 wt % the last band is moved to higher wavenumbers after reduction at higher temperature (773 K).

In the spectra of $Pt/CeO_2-Al_2O_3$ samples calcined at 1073 K and then reduced at 773 K (Figure 7C), the following observations can be detected: (i) the position of the main 2065 cm^{-1} band is unchanged for the sample with 12 wt % CeO_2; (ii) there is a great shift in the main band for the sample with 3 wt % CeO_2 to higher wavenumbers (to 2080 cm^{-1}); (iii) the main band at 2046 cm^{-1} for the Pt/Al_2O_3 sample does not change, but a small new band at 2090 cm^{-1} appears after the calcination at higher temperature; (iv) the main band in the spectra of the samples containing CeO_2 shows a broadening on the low-frequency side.

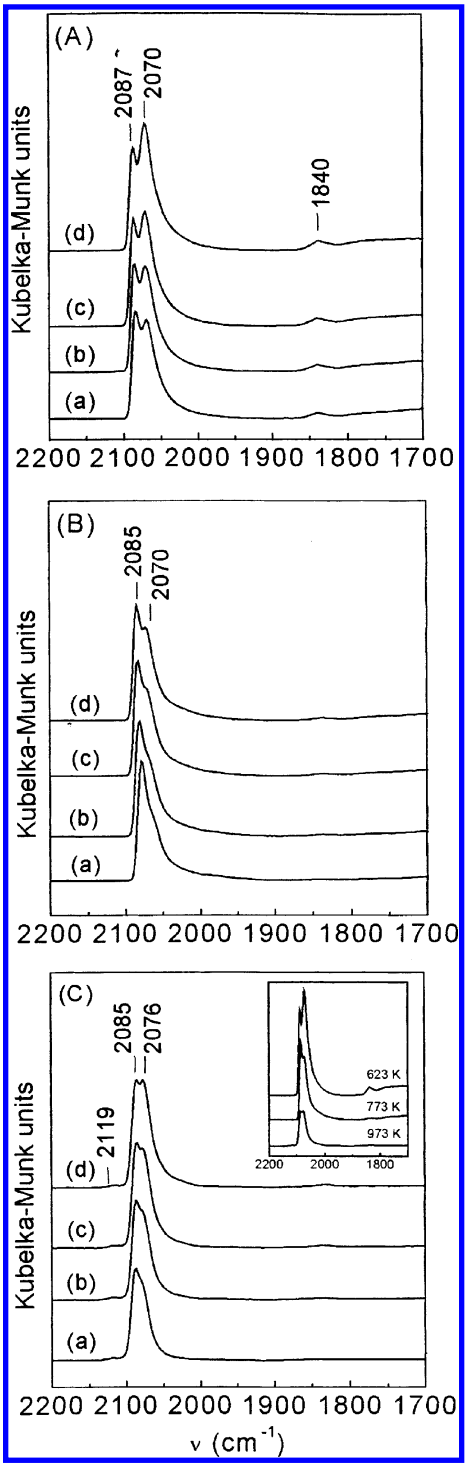

Figure 6. IR spectra of CO adsorption on Pt/CeO_2 reduced at 623 K (A), 773 K (B), and 973 K (C) under different pressures: 0.665 (a), 1.33 (b), 2.00 (c), and 2.66 (d) kPa.

4. Discussion

4.1. Influence of the CeO_2 Loading and the Presence of Pt on the Surface State of Cerium in the $Pt/CeO_2-Al_2O_3$ System Investigated by XPS. Despite the difficulties of interpretation, some clear conclusions can be drawn from

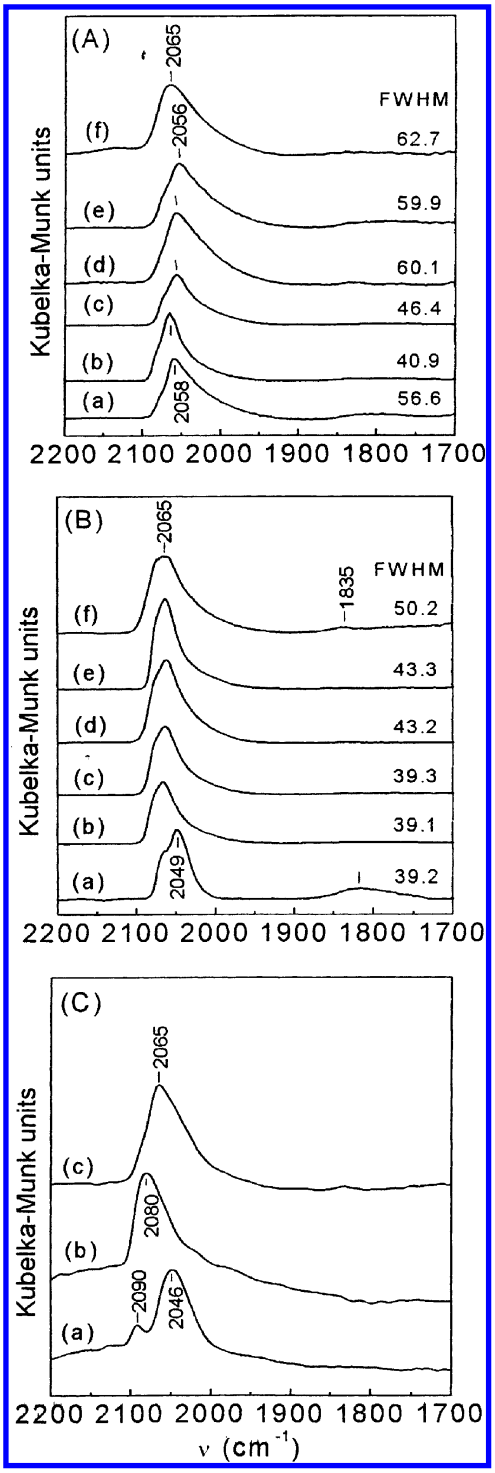

Figure 7. IR spectra of CO adsorption on $Pt/CeO_2-Al_2O_3$ samples with different CeO_2 loadings reduced at 623 K (A) and 773 K (B) under a CO pressure of 2.66 kPa. IR spectra of CO adsorption on samples previously calcined at 1073 K and reduced at 773 K (C). (A, B) 0 (a), 0.5 (b), 1 (c), 3 (d), 6 (e), and 12 (f) wt % CeO_2. (C) 0 (a), 3 (b), and 12 (c) wt % CeO_2.

spectroscopic investigation of cerium-based catalysts. Whether the sample is $Pt/CeO_2-Al_2O_3$ or $CeO_2-Al_2O_3$ carriers[28] in oxidized or reduced form, it is obvious that the cerium at low content (0.5−3 wt %) is in a strongly reduced state (III). This strongly supports the idea of the occupation of an Al(III) cationic state in the first layers by supported Ce(III) cations. Despite the difference in ionic radii (1.03 Å for Ce(III) and 0.50 Å for Al(III)), $CeAlO_3$ can be formed.[51−52] On the other hand, Ce(III) cations would occupy vacant octahedral coordinated sites on the surface of alumina and block the transition of Al(III) cations from tetrahedral to octahedral sites during high-temperature treatment, which caused the loss of the surface area of alumina, as previously shown in ref 28.

In $CeO_2-Al_2O_3$ carriers with CeO_2 loading ≥3 wt %, cerium was always in a higher oxidation state, as observed in our previous work,[28] due to the growth of CeO_2 crystallites. However, the cerium on the surface of these crystallites is in a more reduced state in the presence of Pt, being seen in Figure 2A. The same has been observed for other noble-metal-containing CeO_2 systems.[43] The more reduced state of Ce in the oxide $Pt/CeO_2-Al_2O_3$ system should be related to (i) an electron transfer between Ce and Pt atoms and/or (ii) formation of oxychloride ($Ce^{III}OCl$) or hydroxychloride ($Ce^{III}(OH)_2Cl$) compounds on the surface,[38] caused by the precursor salt of Pt, the calcination temperature of 773 K not being enough to decompose these species. It can be assumed that cerium in oxide $Pt/CeO_2-Al_2O_3$ samples with higher CeO_2 loading is in a mixed oxidation state: (i) oxidation state IV, due to the formation of large three-dimensional CeO_2 or other mixed cerium oxides[40] (Ce_nO_{2n-2}, $n \geq 4$) on the surface of alumina, and (ii) oxidation state III on the surface of these patches, caused by the interaction with Pt and formation of stable cerium oxychloride surface species at 773 K. The absence of agglomerated Pt in Pt/CeO_2 and the presence of very small traces of agglomerated Pt on the $Pt/CeO_2-Al_2O_3$ sample with the highest CeO_2 loading (12 wt %) after calcination at 1073 K (Figure 1C) suggest that the chlorine-containing compounds are still present and/or a strong interaction between the surface of CeO_2 crystallites and Pt exists.

The reduction of $Pt/CeO_2-Al_2O_3$ samples under hydrogen leads to a change in the XPS spectra of Ce 3d core electron levels, as is observed in Figure 2B. The oxidation state of cerium becomes approximately the same for all samples (III). However, in the reduced Pt/CeO_2 sample and the $12CeO_2-Al_2O_3$ carrier, the v^{II} component does not totally disappear after reduction, signifying the presence of cerium in a higher oxidation state (IV). At the same time, in the spectrum of a Pt-containing sample supported on $12CeO_2-Al_2O_3$ carrier the v^{II} component is not observed. Therefore, the reduction of cerium in the $CeO_2-Al_2O_3$ carrier is more difficult than in the Pt-containing $CeO_2-Al_2O_3$ sample with the same CeO_2 loading (higher percentage of u^{III} for $12CeO_2-Al_2O_3$ (Figure 3)). This fact points out the importance of the presence of a transition metal in the reduction process. It has been reported that well-dispersed Pd particles on ceria can easily favor the hydrogen spillover on the support that causes the reduction of cerium oxide[53] and/or formation of $Ce(OH)_3$ species on the surface, which are stable under reducing conditions.[54]

4.2. Electronic and Particle Morphology Effects in CO Infrared Studies. The difference between the IR spectra of Pt/CeO_2 and Pt/Al_2O_3 samples shows that the carrier material (CeO_2, Al_2O_3) influences in different ways the crystal surface structure of Pt, as well as the interaction between the Pt and its support. Studying the CO adsorption on Pt supported on different supports, such as Al_2O_3 and SiO_2, Stoop et al.[55] has observed only one band at 2073 cm^{-1} for Pt/SiO_2 due to one kind of morphology of Pt crystallites present on the surface, owing to the inertness of the silica support. However, for Pt/Al_2O_3, an additional high-wavenumber shoulder at 2080 cm^{-1} was detected, which was related to CO adsorption on the most densely packed planes.[55]

The peak positions of the different CO adsorption bands correspond to different adsorbed CO species. The broader IR spectra of Pt/Al_2O_3 at 623 K (Figure 5A) can be related to

adsorption of CO molecules in a heterogeneous manner on Pt atoms; i.e., there are different factors which influence the change in the electron density of the transition metal. As was shown above Cl^- ions were detected by XPS in the samples calcined and reduced at 773 K. The presence of Cl^- ions could lead to a change in the electronic state of platinum, by interaction with electronegative Cl atoms, which act as electron acceptors; the electron density of the metal d orbital decreases, thus shifting the CO bands to higher frequency. Therefore, the slightly revealed shoulder at about 2080 cm^{-1} would be connected with the strong interaction between Pt and Cl^- ions. The second type of electronic effect occurring on the surface of the Pt/Al_2O_3 sample would be related to the morphology of the metal particles and the structure of the metal surface exposed as suggested in the Blyholder model,[56] which predicts that the different morphologies of metal Pt particles lead to an electronic effect. Two different chemisorbed states for CO adsorbed on the surface of a highly stepped Pt(321) surface have been detected and assigned to adsorption on step and terrace sites, with adsorption energies of 151 and 96 kJ/mol, respectively.[57]

The variation with CO coverage in the intensity and position of the main bands for the Pt/Al_2O_3 sample reduced at the lower temperature (623 K) shows that the lower-frequency band at 2047 cm^{-1} would be associated with adsorption on the steps and the higher-frequency band, at 2060 cm^{-1}, with adsorption on the terraces, according to Tanaka et al.[23] According to Greenler et al.,[58] CO is initially adsorbed on the step sites, with a band at lower frequency; only when the edge is saturated does CO adsorption take place on the terrace sites. At low CO coverage no band characteristic of bridge-bonded species was found, since the stepped sites do not give rise to a bridging species.[58] However, with increasing CO coverage the small band at about 1817 cm^{-1}, related to bridge-bonded CO species, appeared, which is an indication of an increased electron density on the metal particles according to Menacherry et al.[59] Therefore, adsorption preferentially takes place on steps at low CO coverage. CO begins to populate the terraces with increasing CO coverage. The bands of the two species (terraces and steps) are not well resolved at 2.66−5.32 kPa (Figure 5A), probably due to the participation of the dipole−dipole coupling effect. The presence of CO bonded to the steps can be concluded from the asymmetry of the band, which exhibits a broadening on the low-frequency side (Figure 5A). It can be concluded that there are two types of CO adsorption sites, with domination of terrace sites after reduction of the Pt/Al_2O_3 sample at 623 K and at higher CO coverage.

The lowering of the frequency of the main band in the spectra of Pt/Al_2O_3 with increasing temperature of reduction (Figure 5B) can be explained by the influence of two phenomena: (i) competition of metal d electrons for the back-donation and (ii) the extent of the dipole−dipole coupling.[58] An experimental study of CO adsorption on Pt(111) by Crossley et al.[60] led to the conclusion that the 35 cm^{-1} frequency shift with increasing CO coverage can be attributed to coupling. Contrary to that, Primet,[22] studying CO adsorption by isotopic dilution experiments (using a mixture of $^{12}CO-^{13}CO$), showed that the shift of the main band to a lower frequency of 28 cm^{-1} can be explained by a decrease in the dipole−dipole coupling due to the separation of the CO dipoles caused by dilution with ^{13}CO molecules. The same conclusion has been reached in other papers, which stresses the importance of dipole−dipole coupling in the spectra of CO adsorption on a metal.

According to the classic model of Blyholder[56] of the bonding of CO molecules to metal surfaces in small platinum particles, the average number of platinum bonds per platinum atom is lower than in larger particles; therefore, a higher metal electron density is available for back-donation into the 2π orbital of CO molecules, leading to a decrease in the C−O bond strength and a lowering of the CO adsorption frequency.

The relative consistency in peak positions and the narrowness of the CO adsorption peaks, after reduction of Pt/Al_2O_3 at 773 K (Figure 5B), would be related to a change in the electronic state of platinum. Since the integrated absorbance of adsorbed CO remains almost constant, the observed shift to lower frequency in Pt/Al_2O_3 reduced at higher temperature (773 K) (Figure 5B) can be attributed to a subsequent reduction of partially oxidized $Pt^{\delta+}$ atoms present at the lower temperature of reduction. It has been reported that the reduction of $Pt-O_x$ species proceeds at lower temperatures than that of chlorinated species in Pt-supported catalysts ($PtCl_xO_y$ species).[61] The frequency downshift is connected with increasing electron density of metal Pt particles, i.e., fully reduced Pt. The appearance of a highly intensive band at 1816 cm^{-1} suggests the presence of atoms with high electron density, as was suggested by Smoluchowski's theory.[62]

The higher values of the IR bands for Pt/CeO_2 reduced at all temperatures (Figure 6) could be related to (i) a strong interaction between Pt and CeO_2 support and/or chlorine ions and (ii) the presence of different morphologies of Pt particles. It should be noted that the electronic effect can be either caused by a metal−support interaction, involving charge electron transfer between the metal particles and the support, or related to the specific morphologies of the metal particles formed on the supports on using different temperatures of reduction. It is unlikely that charge transfer from the CeO_2 support to the metal particles takes place at the lower temperature of reduction (623 K) for the increased electron density of the metal particles on Pt/CeO_2 compared to those reduced at higher temperatures. A more likely explanation is that the metal particles have more coordinatively unsaturated surface atoms. The Pt/CeO_2 samples reduced at 623 K show a strong band at 2070 cm^{-1} and an increase in the ratio of bridged to linear CO species that is consistent with an increase in the electron density of the metal particles (Figure 6A). As is noted in Figure 6A,B, the positions of CO adsorption bands with high frequencies are the same, suggesting that the CO adsorption sites are the same on these catalysts. However, the intensity of the high-frequency band at 2085 cm^{-1} is higher than that at 2070 cm^{-1}. The bridge-bonded CO species practically disappears in the spectra of Pt/CeO_2 reduced at 773 K. This means that the electron density of the metal particles decreases at the higher temperature of reduction. At the highest temperature of reduction (973 K) there is no change in the position of the higher-frequency band, but its intensity becomes similar to that of the lower-frequency band. At the same time, the latter band is shifted to higher frequency (to 2076 cm^{-1}). This similarity in the intensity of both bands and the approximation of the position of the bands at 973 K, i.e., the inversion of these bands, give strong evidence of origination from geometrically the same active sites.

From a comparison of the present data with those of other workers we can conclude that the origin of the IR bands is related to adsorbed CO molecules in different local environments, due to the size/shape distribution of Pt particles on the surface. When the theory of Smoluchowski[62] is applied to chemisorption of CO, one expects that the back-donation from the metal will be lower for protruding atoms, e.g., at corners, than for atoms in terraces of Pt crystal surfaces. Therefore, the linear mode of adsorbed CO with high stretching frequency is

prevailed on protruding atoms in Pt/CeO_2 samples at all temperatures of reduction.

The intensity of all bands decreases with increasing temperature of reduction (Figure 6C), meaning that the higher temperature of reduction inhibits the platinum chemisorption capability, due to a decoration phenomenon caused by the SMSI.[16] The electronic effect, produced by the SMSI between Pt and CeO_2 during reduction, leads to formation of reduced support species (CeO_x), which migrate onto the Pt particles, causing a loss of the chemisorption properties of the metal. Most probably, the "dilution" effect of the reduced CeO_x species is responsible for the decrease of the difference between the different planes of Pt, so that the distribution of Pt species on the catalyst surface becomes more uniform. The latter is supported by disappearance of the 1840 cm^{-1} band, related to CO bridge-bonded to Pt atoms, at a higher temperature of reduction. Therefore, the importance of the electronic effect becomes greater compared to that of the geometric effect at reduction temperatures >773 K, in agreement with Tanaka et all.[23]

Since the position of the higher-frequency band at 2087 cm^{-1} did not change during reduction, at all temperatures it can be associated with the adsorption of CO on a single Pt atom in contact with Cl^- ions and/or with oxygen according to Daniel,[14] while the lower-frequency band can be associated with CO adsorption on Pt without oxygen and/or Cl^- ions. However, both bands represent CO adsorption at geometrically similar sites. It has been shown by O_2 adsorption studies on single Pt crystals that oxygen is preferentially adsorbed on step or kink surface sites.[63]

The IR results indicate that both the morphology of the metal particles and the electronic effect, in Ce-modified alumina-supported Pt, are strongly influenced by the support and by the different loadings of CeO_2 on the alumina surface (Figure 7). All the $Pt/CeO_2-Al_2O_3$ samples with CeO_2 loadings between 1 and 6 wt % at 623 K have similar CO absorption bands (Figure 7A), suggesting that the surface sites for the adsorption of CO are similar over these samples. Comparing the spectrum of the $Pt/CeO_2-Al_2O_3$ sample with the lowest CeO_2 loading (0.5 wt %) with those of samples with 1−6 wt % CeO_2, it is seen that the increasing CeO_2 loading causes a shift of the CO adsorption bands to lower frequency (from 2065 to 2056 cm^{-1}) as well as an increase of the asymmetry of the main band on the low-frequency side. These phenomena can be connected with the presence of metal particles with different electron densities, but the difference between them is not larger. The latter can be related to the presence of small Pt crystallites, which have a larger fraction of defect sites. The very weak band at 1840 cm^{-1} related to bridge-bonded Pt in the spectra of the samples with 3−6 wt % CeO_2 means an increase in the electron density of Pt. The absence of this band in the case of the supported Pt sample with 1 wt % CeO_2 means a more uniform distribution of steps or corner sites present on the surface. A more uniform size distribution of Pt is present in the sample with the lowest CeO_2 loading (0.5 wt %); the higher-frequency band position can be connected with the presence of more coordinatively unsaturated Pt, caused by a stronger interaction between Pt and Ce (Table 1) as well as between Pt and Cl^- ions. The same can be said for the sample with the highest CeO_2 loading; the presence of higher unsaturated Pt atoms predominates.

Increasing the reduction temperature up to 773 K of $Pt/CeO_2-Al_2O_3$ samples leads to a more uniform size distribution of Pt with lower electron density (Figure 7B), which could be caused by more intimate contact between Pt and CeO_2.

Comparing the spectra of Ce-containing Al_2O_3-supported Pt samples with that for the Ce nonpromoted sample, a great shift in the position of the main band is observed (from 2058 to 2065 cm^{-1} and from 2049 to 2066 cm^{-1} at 623 and 773 K reduction, respectively) (Figure 7A,B). The shift in the band position as well as the change in the fwhm could be mainly connected with the different electron densities of Pt atoms, due to (i) the different reduction temperatures in the sample pretreatments, (ii) the influence of CeO_2 loading, and/or (iii) the presence of interaction between Pt and the Ce-modified support.

The effect of the calcination temperature on the CO chemisorption properties of Pt particles is very well seen when the spectra of the samples calcined at 1073 K (Figure 7C) are compared with those for the samples calcined at 773 K (Figure 7B). As seen by XRD, the calcination in air flow at 1073 K (Figure 1B) leads to agglomeration of Pt particles on Al_2O_3 and on low-CeO_2-loaded samples, due to the decomposition of the PtO_xCl_y complex formed during preparation of the samples. The upshift of the frequency band for Pt/Al_2O_3 and $Pt/CeO_2-Al_2O_3$ with 3 wt % CeO_2 would be mainly related to (i) the decrease in the electron density of supported transition metal, due to the absence of electronegative Cl^- ions, and (ii) the strong interaction of Pt with oxygen from the support and formation of highly unsaturated Pt atoms.

5. Conclusions

The spectral characterization of Pt supported on Al_2O_3, CeO_2, and mixed $CeO_2-Al_2O_3$ oxides with different CeO_2 loadings shows the great influence of the type of the support and pretreatment temperature on the surface state of Pt and Ce.

Different oxidation states of Ce are observed for calcined samples: (i) Ce(III) up to ≤3 wt % and (ii) Ce(III) and Ce(IV) at higher CeO_2 loadings. The oxidation state of cerium becomes approximately the same for all reduced samples, Ce(III).

Pt is well dispersed in all samples calcined at 773 K, as revealed by the absence of XRD patterns. On increasing the temperature of calcination to 1073 K there is agglomeration of Pt on Al_2O_3 and low-CeO_2-loaded samples, due to the decomposition of the PtO_xCl_y complex. XPS data show that Pt in the samples reduced at 773 K maintains some positive character due to the more intimate contact between Pt and Ce.

The IR results for adsorbed CO suggest that the morphology of the metal particles, as well as the electronic effect, in supported Pt samples is strongly influenced by the type of support and temperature of reduction.

Increasing the reduction temperature to 773 K leads to a more uniform distribution of coordinatively unsaturated Pt atoms on the surface of Pt/Al_2O_3 modified with ceria.

The highest reduction temperature for the Pt/CeO_2 sample (973 K) inhibits the Pt chemisorption capability for CO adsorption, due to the geometric effect of reduced CeO_x species.

Acknowledgment. We are grateful for the financial support of FAPESP (Fundação para o Amparo a Pesquisa do Estado de São Paulo; Grant No. 01/10655-7), CAPES (Coordenação de Aperfeiçoamento de Pessoal de Nível Superior), and Petrobras.

References and Notes

(1) Yao, H. C.; Yao, Y. F. Y. *J. Catal.* **1984**, *86*, 254.
(2) Leitenburg, C.; Trovarelli, A.; Kaspar, J. *J. Catal.* **1997**, *166*, 98.
(3) Trovarelli, A. *Catal. Rev.—Sci. Eng.* **1996**, *38*, 439.
(4) Trovarelli, A.; De Leitenburg, C.; Boaro, M.; Dolceti, G. *Catal. Today* **1999**, *50*, 453.
(5) Cheng, W. C.; Kim, G.; Petrs, A. W.; Zhao, X.; Rajagopalan, K. *Catal. Rev.—Sci. Eng.* **1998**, *40*, 39.

(6) Pantu, P.; Gavalas, G. R. *Appl. Catal., A* **2002**, *223*, 253.
(7) Pino, L.; Recupero, V.; Beninati, S.; Shukla, A. K.; Hegde, M. S.; Bera, P. *Appl. Catal., A* **2002**, *225*, 63.
(8) Otsuka, K.; Wang, Y.; Sunada, E.; Yamanaka, I. *J. Catal.* **1998**, *175*, 152.
(9) Ruckenstein, E.; Wang, H. Y. *J. Catal.* **1999**, *187*, 151.
(10) Bernal, S.; Botana, F. J.; Calvino, J. J.; Cifredo, G. A.; Pérez-Omil, J. A.; Pintado, J. M. *Catal. Today* **1995**, *23*, 21.
(11) Bernal, S.; Calvino, J. J.; Gatica, J. M.; Larese, C.; Lopez-Cortez, C.; Perez-Omil, J. A. *J. Catal.* **1997**, *169*, 510.
(12) Martinez, A.; Fernandez-Garcia, M.; Salamanca, L. N.; Valenzuela, R. X.; Conesa, J. C.; Soria, J. *J. Phys. Chem. B* **2000**, *104*, 4038.
(13) Jin, T.; Zhou, Y.; Mains, G. J.; White, M. *J. Phys. Chem.* **1987**, *91*, 5931.
(14) Daniel D. W. *J. Phys. Chem.* **1988**, *92*, 3891.
(15) Holmgren, A.; Anderson, B.; Duprez, D. *Appl. Catal., B* **1999**, *22*, 215.
(16) Bernal, S.; Blanco, G.; Gatica, J. M.; Larese, C.; Vidal, H. *J. Catal.* **2001**, *200*, 411.
(17) Tiernan, M. J.; Finlayson, O. E. *Appl. Catal., B* **1998**, *19*, 23.
(18) Cracium, R.; Daniell, W.; Knözinger, H. *Appl. Catal., A* **2002**, *230*, 153.
(19) Yamaguchi, T.; Ikeda, N.; Hattori, H.; Tanabe, K. *J. Catal.* **1981**, *67*, 324.
(20) Engler, B.; Koberstein, E.; Schubert, O. *Appl. Catal.* **1989**, *48*, 71.
(21) Primet, M.; Basset, J. M.; Mathieu, M. V.; Prettre, M. *J. Catal.* **1973**, *29*, 213.
(22) Primet, M. *J. Catal.* **1984**, *88*, 273.
(23) Tanaka, K.; White, J. M. *J. Catal.* **1983**, *79*, 81.
(24) Sheu, L. L.; Karpinski, Z.; Sachtler, W. M. H. *J. Phys. Chem.* **1989**, *93*, 4890.
(25) Portugal, U. L.; Marques, C. M. P.; Araujo, E. C. C.; Morales, E. V.; Giotto, M. V.; Bueno, J. M. C. *Appl. Catal., A* **2000**, *193*, 173.
(26) Portugal, U. L.; Santos, A. C. S. F.; Damyanova, S.; Marques, C. M. P.; Bueno, J. M. C. *J. Mol. Catal.* **2002**, *184*, 311.
(27) Gheno, S. M.; Damyanova, S.; Riguetto, B. A.; Marques, C. M. P.; Bueno, J. M. C. *J. Mol. Catal. A* **2003**, *198*, 263.
(28) Damyanova, S.; Perez, C. A.; Schmal, M.; Bueno, J. M. C. *Appl. Catal., A* **2002**, *234*, 271.
(29) Scofield, H. J. *J. Electron Spectrosc. Relat. Phenom.* **1976**, *8*, 129.
(30) Fathi, M.; Bjogum, B.; Viig, T.; Rokstad, O. K. *Catal. Today* **2000**, *63*, 489.
(31) Lietz, G.; Lieske, H.; Spindler, H.; Hanke, W.; Völter, J. *J. Catal.* **1983**, *81*, 17.
(32) Wuilloud, E.; Delley, B.; Schneider, W. D.; Baer, Y. *Phys. Rev. Lett.* **1984**, *53*, 202.
(33) Plateau, A.; Johnsson, L. I.; Hagström, A. L.; Karisson, S. E. *Surf. Sci.* **1997**, *63*, 153.
(34) Fujimori, A. *Phys. Rev. B* **1983**, *27*, 3992.
(35) Kotani, A.; Mizuta, H.; Jo, T.; Parlebas, J. C. *Solid State Commun.* **1985**, *53*, 805.
(36) Krill, G.; Kappler, J. P.; Meyer, A.; Abadli, L.; Ravet, M. F. *J. Phys. F* **1981**, *11*, 1713.
(37) Shyu, J. Z.; Weber, W. H.; Gandhhi, H. S. *J. Phys. Chem.* **1988**, *92*, 4964.
(38) Kondarids, D. I.; Verykios, X. E. *J. Catal.* **1998**, *174*, 52.
(39) Shyu, J. Z.; Otto, K. *J. Catal.* **1989**, *115*, 16.
(40) Normand, F. L.; Hilaire, L.; Kili, K.; Krill, G.; Maire, G. *J. Phys. Chem.* **1988**, *92*, 2561.
(41) Shyu, J. Z.; Otto, K. *Appl. Surf. Sci.* **1988**, *32*, 246.
(42) Vedrine, J. C.; Dufaux, M.; Naccache, C.; Imelik, B. *J. Chem. Soc., Faraday Trans. 1* **1978**, *74*, 440.
(43) Jackson, S. D.; Willis, J.; McLellan, G. D.; Webb, G.; Keegan, M. B. T.; Moyes, R. B.; Simpson, S. Wells, P. B.; Whyman, R. *J. Catal.* **1993**, *139*, 191.
(44) Lieske, H.; Lietz, G.; Spindler, H.; Völter, J. *J. Catal.* **1983**, *81*, 8.
(45) Binet, C.; Badri, A.; Boutonnet-Kizling, M.; Lavalley, J. C. *J. Chem. Soc., Faraday Trans.* **1997**, *90* (7), 1023.
(46) Li, C.; Sakata, Y.; Arai, T.; Domen, K.; Maruya, K.; Onishi, T. *J. Chem. Soc., Faraday Trans. 1* **1989**, *85*, 92.
(47) Barth, R.; Pitchai, R.; Anderson, R. L.; Verykios, X. E. *J. Catal.* **1989**, *116*, 61.
(48) Jackson, S. D.; Glanville, B. M.; Willis, J.; McLellan, G. D.; Web, G.; Moyes, R. B.; Simpson, S.; Wells, P. B.; Whyman, R. *J. Catal.* **1993**, *139*, 207.
(49) Dulaurent, O.; Bianchi, D. *Appl. Catal., A* **2000**, *196*, 271.
(50) Xu, J.; Yates, J. T. *Surf. Sci.* **1995**, *327*, 193.
(51) Tanaka, K.; White, J. M. *J. Phys. Chem.* **1982**, *86*, 3977.
(52) Kim, Y. S. *Acta Crystallogr., Sect. B: Struct. Crystallogr. Cryst. Chem.* **1968**, *24*, 295.
(53) Bernal, B.; Calvino, J. J.; Cifredo, C. A.; Rodriguez-Izquierdo, J. M.; Perrichon, V.; Laachir, A. *J. Catal.* **1992**, *1*, 147.
(54) Barbezat, S.; Loriers, J. *C. R. Acad. Sci.* **1952**, *234*, 1978.
(55) Stoop, F.; Toolenaar, F. J. C. M.; Ponec, V. *J. Catal.* **1982**, *73*, 50.
(56) Blyholder, G. *J. Phys. Chem.* **1964**, *68*, 2772.
(57) McClellan, M. R.; Gland, J. L.; McFeeley, F. R. *Surf. Sci.* **1981**, *112*, 63.
(58) Greenler, R. G.; Burch K. D.; Kretzschmar, K.; Klauser, R.; Bradshaw, A. M. *Surf. Sci.* **1985**, *152*/*153*, 338.
(59) Menacherry, P. V.; Haller, G. L. *J. Catal.* **1998**, *177*, 175.
(60) Crossley, A.; King, D. A. *Surf. Sci.* **1977**, *68*, 528.
(61) Contescu, C.; Macovei, D.; Craiu, C.; Teodorescu, J. A.; Schwarz, J. A. *Langmuir* **1995**, *11*, 2031.
(62) Smoluchowski, R. *Phys. Rev*. **1941**, *60*, 661.
(63) Ducros, R.; Merril, R. P. *Surf. Sci.* **1976**, *55*, 227.